Calculated Quantizing Noise of Single-Integration Delta-Modulation Coders

By J. E. IWERSEN

(Manuscript received March 28, 1969)

We calculate the granular quantizing noise for a delta modulator that has unequal positive and negative step sizes. The asymmetry leads to a highly colored noise spectrum. We perform this calculation by adding a ramp function of time to the input of a symmetrical coder. The resulting formulas can also be used for uniform DPCM and PCM coders. The idle-channel spectrum consists of discrete lines which scatter somewhat irregularly in amplitude and frequency; they can be regarded as the result of sampling (aliasing) a sawtooth wave. These lines are phase-modulated by a coder input. For a sinusoidal input, discrete side frequencies are produced which again have an irregular progression of amplitudes. Gaussian inputs lead to gaussian line shapes; the lines broaden as input power is increased. A totally white spectrum (as is often assumed in connection with delta-modulation-system considerations) cannot be attained, however, before the onset of slope overload. We give a numerical example that uses a coder suitable for telephone applications. One can see that step asymmetry can be very advantageous in attaining low noise.

I. INTRODUCTION

While Laane and Murphy[1] were investigating the encoding of speech using delta modulation ($\triangle$M)[2] it became apparent to us that existing theories of granular quantizing noise[3,4] were seriously deficient; they did not take into account, except in a very elementary way, the asymmetry of the positive and negative integrator step sizes. This work intends to correct this deficiency.

Figure 1 is a block diagram of a $\triangle$M coder-decoder. An input signal is compared with a locally reconstructed version of itself and the differential, or error, is quantized into a one-bit code, transmitted, and integrated at a receiver to recover the original signal. Quantizing noise is produced by the coding process and is also recovered at the

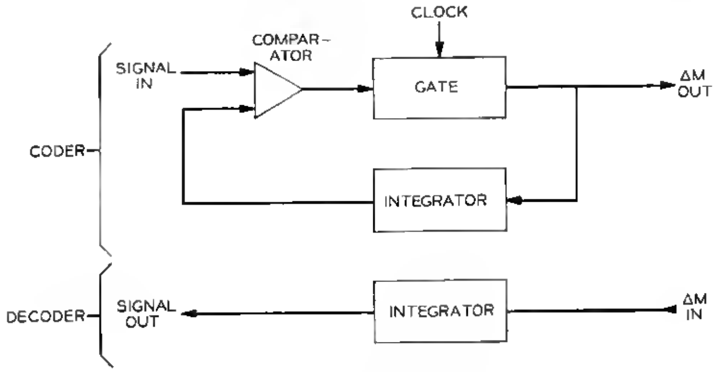

Fig. 1 — Delta-modulation coder plus decoder (codec).

receiver; this noise is the subject of this paper. We limit our consideration to single-integration systems.

In the past, considerations of ΔM noise have been broken into two distinct areas: calculation of quantizing noise accompanying a typical signal,[3] and calculation of idle-channel (zero-input-signal) noise.[4] As Fig. 2 shows, there is no idle-channel noise for a coder in which the plus and minus quanta (steps) fed to the integrator are exactly equal in magnitude. The integrator output spectrum contains only the out-of-signal-band Nyquist frequency, f_N (one half the sampling frequency, f_s) and its harmonics. In any real coder, however, it is impossible to balance the plus and minus steps perfectly, with the result that the output contains occasional double-plus (or double-minus) steps, as Fig. 3 shows. In general, this waveform has signal-band components. Wang calculated the noise for this case but his results, while adequate as far as they go, are incomplete and nonrigorous.[4] Van de Weg's calculation of noise in the presence of signal was for an equal-step (symmetrical) coder.[3] We do the calculation for an unequal-

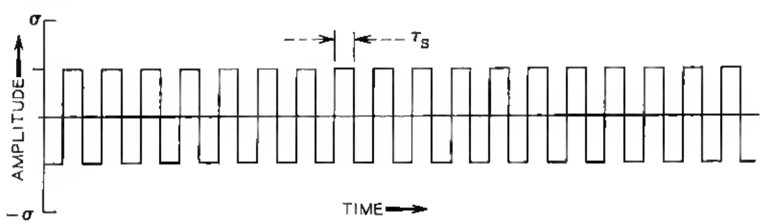

Fig. 2 — Integrator-output wave from a symmetrical (equal-step-size) coder.

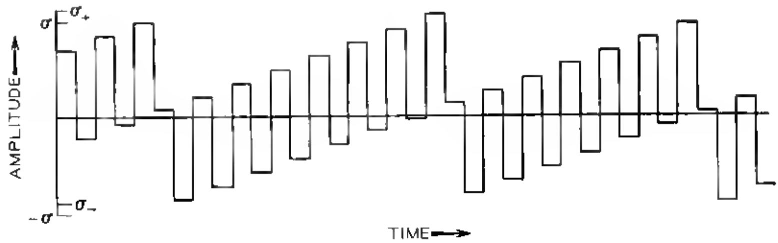

Fig. 3 — Integrator-output wave from an asymmetrical (unequal-step-size) coder, shown with $|\sigma_+| > |\sigma_-|$.

step (asymmetrical) coder and show that there are significant differences.

In much of the literature on delta modulators, where noise is treated casually, the assumption is made that the total average noise power is more or less uniformly distributed in the band from zero frequency to the Nyquist frequency. This assumption is a very good approximation for multibit PCM and DPCM but, as we show, can lead to colossal errors for ΔM.

Results presented for gaussian input are in terms of time-averaged noise power. In this form they are directly useful for speech systems and typical data systems but are of more limited value for video systems, where details of the waveform are perceived.

In Sections II and III, we set up the method of attacking the problem. Then in Section IV we treat zero input (the idle channel), in Section V a sinusoidal input, and in Section VI a broadband gaussian input. The appendixes contain various mathematical developments necessary for logical completeness but not important to the reader interested in engineering understanding and application of the main results (with the possible exception of Appendix D).

II. QUANTIZING RULES

The function of the coder (Fig. 1) is, at each clock time or sampling instant, to add a positive step (σ_+) to the integrator output (q) if this output is less than the signal input (y) or to add a negative step (σ_-) if the output is greater than the input. If the integrator has instantaneous response and infinite time constant, the output is a sequence of rectangular pulses, as in Figs. 2 and 3.

If y_n is the value of the input at the nth sampling instant, and q_n is the output value just before this instant, the operation can be sum-

marized:

$y_n - q_n$	q_{n+1}
$+$	$q_n + \sigma_+$
$-$	$q_n + \sigma_-$

As we mentioned, it is not possible to make the magnitudes of σ_+ and σ_- exactly equal in a real coder. Let us therefore define

$$\sigma_+ \equiv \sigma + \epsilon, \qquad \sigma_- \equiv -\sigma + \epsilon, \tag{1}$$

where σ, the average step size, is a positive quantity. The coder operation can then be summarized in a single equation:

$$q_{n+1} = q_n + \sigma \operatorname{sgn}(y_n - q_n) + \epsilon. \tag{2}$$

We are actually interested in the error, or noise, $x \equiv q - y$, which accompanies the reconstructed signal. (Appendix A shows that x is usually uncorrelated with y and is therefore noise under any circumstances.) Substituting for q in equation (2) gives the noise as a function of the input:

$$x_{n+1} - x_n + \sigma \operatorname{sgn} x_n = -y_{n+1} + y_n + \epsilon \tag{3}$$

$$= -[y_{n+1} - (n+1)\epsilon] + [y_n - n\epsilon] \tag{4}$$

$$\equiv -y'_{n+1} + y'_n\,. \tag{5}$$

Thus we are led to a crucial principle: *The noise output of an asymmetrical ($\epsilon \neq 0$) ΔM coder can be calculated as the noise output of a symmetrical ($\epsilon = 0$) coder, if the input is taken as the actual input plus an appropriate ramp or staircase function of time.*

If equation (5) is summed from $t = -\infty$ to just before the nth instant [assuming $x(-\infty) = y(-\infty) = 0$],

$$x_n + \sigma \sum_{i=-\infty}^{n-1} \operatorname{sgn} x_i = -y'_n \tag{6}$$

or

$$q'_n = -\sigma \sum_{i=-\infty}^{n-1} \operatorname{sgn} x_i\,. \tag{7}$$

The resulting summation in equation (7) must be an integer alternating between odd and even values as a function of n. We can, without loss of generality, take it even for even n. [In equation (11) we include an arbitrary initial value of amplitude for the ramp; this covers the

possibility that the odd-even assumption is consequential.] If we assume that the coder does not go into slope overload (that is the input slope stays between the limits σ_+/τ_s and σ_-/τ_s), then q_n'/σ is the nearest odd integer to $(y_n' + \epsilon)/\sigma$ for the odd sampling instants and the nearest even integer for the even instants. $y_n' + \epsilon$ appears, rather than y_n', because the error must range from $\sigma + \epsilon$ to $-\sigma + \epsilon$ rather than from $+\sigma$ to $-\sigma$. The effect of this added ϵ is simply that the coder transmits a dc level of ϵ in addition to other signals and noise. Since ΔM systems normally suppress dc, as is mentioned in Section III in connection with other reasons, this added ϵ is dropped in the succeeding mathematical development. If it is desired to include it, $x - \epsilon$ should be substituted for x in what follows.

We have seen that a ΔM coder has two quantizing functions which alternate in time. Figures 4 and 5 show these functions; both the input and output are normalized to σ.

$q_0'(y)$ and $q_e'(y)$ were called $E(y)$ and $O(y)$ by van de Weg who cast them into contour-integral form and used them directly.[3] We prefer to follow the suggestion of Rice and use the error functions, $x(y)$, also shown in Figs. 4 and 5.[5] These functions, periodic in y, are conveniently represented by their Fourier series:

$$x_e = \sum_{l\neq 0} \frac{\sigma}{\pi i l} \exp(\pi i l g'), \tag{8}$$

and

$$x_0 = \sum_{l\neq 0} (-1)^l \frac{\sigma}{\pi i l} \exp(\pi i l g') \tag{9}$$

where $g' \equiv y'/\sigma$. For a ΔM coder then,

$$x_n = \sum_{l\neq 0} (-1)^{ln} \frac{\sigma}{\pi i l} \exp(\pi i l g_n') \tag{10}$$

$$= \sum_{l\neq 0} \frac{\sigma}{\pi i l} \exp[\pi i l(n + g_n')] \tag{11}$$

$$= \sum_{l\neq 0} \frac{\sigma}{\pi i l} \exp\{\pi i l[\vartheta_0 + (1 - \vartheta)n + g_n]\}, \tag{12}$$

where we have introduced

$$g_n \equiv \frac{y_n}{\sigma}, \qquad \vartheta = \frac{\epsilon}{\sigma}, \qquad \vartheta_0 = \frac{\epsilon_0}{\sigma}. \tag{13}$$

The last part of equation (13) takes into account an arbitrary initial amplitude for the ramp.

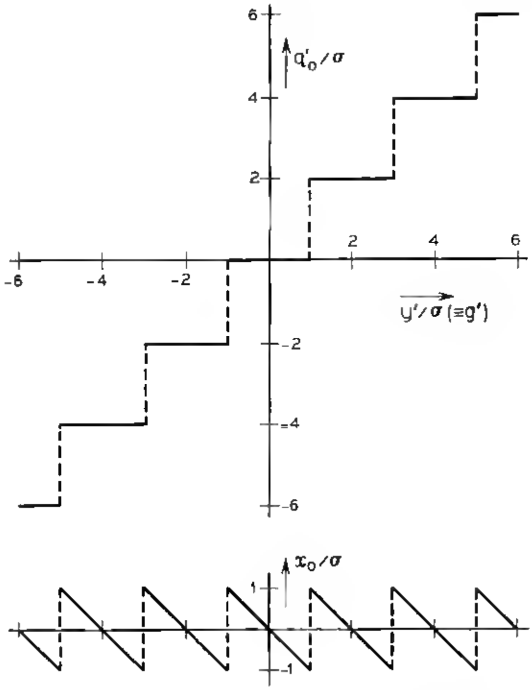

Fig. 4 — Quantizing and error functions for odd sampling intervals.

There is actually nothing in equation (12) which constrains the change in integrator output to be equal to one step per sampling interval. Indeed, the quantizing functions in Figs. 4 and 5 are perfectly valid for uniform DPCM systems where changes $\pm\sigma$, $\pm 3\sigma$, $\cdots$, $\pm(2N - 1)\sigma$ are allowed. Thus the formulas developed in this paper can be used for DPCM (and PCM—see Appendix B) with the provision that they are useful for input signals with up to $2N - 1$ times the maximum slope of the ΔM system. This provision is not trivial, however; when signals range over many steps per sampling interval the errors tend to be uncorrelated, the noise spectrum tends to be white, and the structure (important for ΔM) calculated here is negligible.

III. NOISE FORMULA

Results in this paper are given in terms of frequency spectra of noise (two-sided unless otherwise identified). It is well known that

the spectrum of a pulse sequence can be broken into a factor which contains the information about the pulse shape and a factor which contains information about the area of each pulse and the periodicity. The "shape" factor (called also the "structure" or "aperture" factor) depends on the details of the coder circuit response. This factor is frequently negligible, because the low pass filter it represents normally does not contribute any significant distortion in the signal band. Thus we need only consider a δ-function representation of the sampled-signal, integrator-output, and noise pulse trains, as did van de Weg.[3]

The noise wave with the proper area for each pulse is

$$\nu(t) = \tau_s \sum_{n=-\infty}^{\infty} x_n \, \delta(t - n\tau_s), \tag{14}$$

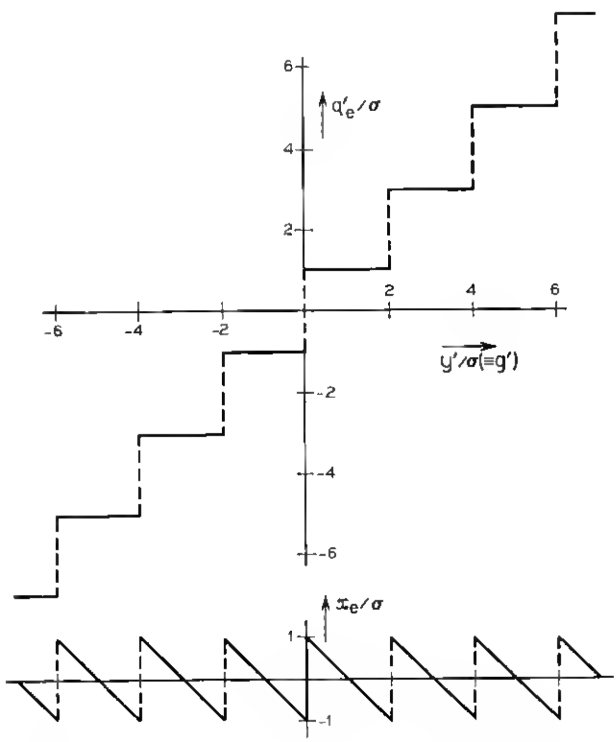

Fig. 5 — Quantizing and error functions for even sampling intervals.

where τ_s is the sampling interval ($\equiv 1/f_s$). If $x(t)$ is defined as a continuous wave with samples $x_n = x(n\tau_s)$, equation (14) can be written

$$\nu(t) = \tau_s x(t) \sum_{n=-\infty}^{\infty} \delta(t - n\tau_s) \tag{15}$$

$$= x(t) \sum_{k=-\infty}^{\infty} \exp(2\pi i k f_s t). \tag{16}$$

A convenient form for $x(t)$ is, using equation (12),

$$x(t) = \sum_{l\neq 0} \frac{\sigma}{\pi i l} \exp\{\pi i l[\vartheta_0 + (1 - \vartheta)f_s t + g(t)]\}, \tag{17}$$

where

$$g(t) \equiv \frac{y(t)}{\sigma}. \tag{18}$$

Combining equations (16) and (17) gives

$$\nu(t) = \sum_{l\neq 0} \sum_{k=-\infty}^{\infty} \frac{\sigma}{\pi i l} \exp\left[\pi i l \vartheta_0 + 2\pi i\left(\frac{l(1-\vartheta)}{2} + k\right)f_s t + \pi i l g(t)\right]. \tag{19}$$

Thus the noise wave (before filtering by the shape factor) consists of a collection of lines of frequency

$$\left(\frac{l(1-\vartheta)}{2} + k\right)f_s ,$$

each phase-modulated by the input signal through a time-dependent angle, $\pi l g(t)$. These lines are examined in Section IV.

It is well known that the power spectrum of equation (14), and therefore equation (19), is periodic in frequency, f, with period f_s. We can thus concentrate on the band from $-f_N$ to f_N. Because of the aliasing or folding problem, all useful signals lie in this band (or any band of width f_s). The total power in $(-f_N, f_N)$ is $\sigma^2/3$, which is also equal to the mean square error, $\langle x^2 \rangle$. Appendix D treats these matters explicitly.

Equation (19) gives the noise generated at the coder, while one is ordinarily interested in the noise at a (distant) decoder. Unless the decoder has exactly the same step sizes as the coder, the noises are different. If the σ's are different, there is some linear gain or loss in the system; signal and noise are affected equally and their ratio, the really significant figure of merit, is not affected. If the ϑ's are different, the noises will differ only by a drift or ramp function of time. To get

rid of this ramp (and also because it is necessary to damp out the effect of errors in transmission) real systems have low-frequency (below-signal-band) cutoffs, called leaks, built into the integrators. The high-frequency cutoffs of the coder and decoder integrators may also be different. In the event that these cutoffs affect the signal band they can be taken into account as separate factors in determining the spectrum. Thus equation (19) can be used to calculate noise at the decoder output.

IV. IDLE-CHANNEL NOISE

The term "idle-channel noise" is used here as if it were synonymous with "zero-input noise." We recognize that this terminology is somewhat loose, in that an idle channel is actually characterized by a thermal or other noise input. Nevertheless, this usage seems established in the literature and the distinction is not significant for most cases of practical interest.

Figure 3 shows the integrator output of an asymmetrical coder. An approximately sawtooth-shaped wave with peak-to-peak amplitude $\approx \sigma$ is clearly visible (Wang's "first envelope function").[4] Other not-so-evident sawteeth are also usually present.

Putting $y = 0$ into equation (4), we see that the idle-channel noise output of an asymmetrical coder can be calculated as the noise output of a symmetrical coder with a ramp input. Figure 6 illustrates this. The error wave in Fig. 6 is the same as the wave in Fig. 3 except for an inconsequential difference in the pulse shapes.

The idle-channel output is calculated by setting $g = 0$ in equation (19):

$$\nu_0(t) = \sum_{l \neq 0} \sum_{k=-\infty}^{\infty} \frac{\sigma}{\pi i l} \exp \left[\pi i l \vartheta_0 + 2\pi i \left(\frac{l}{2} (1 - \vartheta) + k \right) f_s t \right] \tag{20}$$

which describes a collection of discrete lines. Figure 7 shows a number of these lines; the symmetry of the spectrum about all integral multiples of f_N is apparent.

For any given value of l, there is only one value of k which leads to a line in the Nyquist interval $(-f_N, f_N)$. This line, of frequency f_l, can be defined: Let

$$Q(\alpha) = \alpha - N(\alpha) \tag{21}$$

where

$$N(\alpha) = \text{integer nearest } \alpha.$$

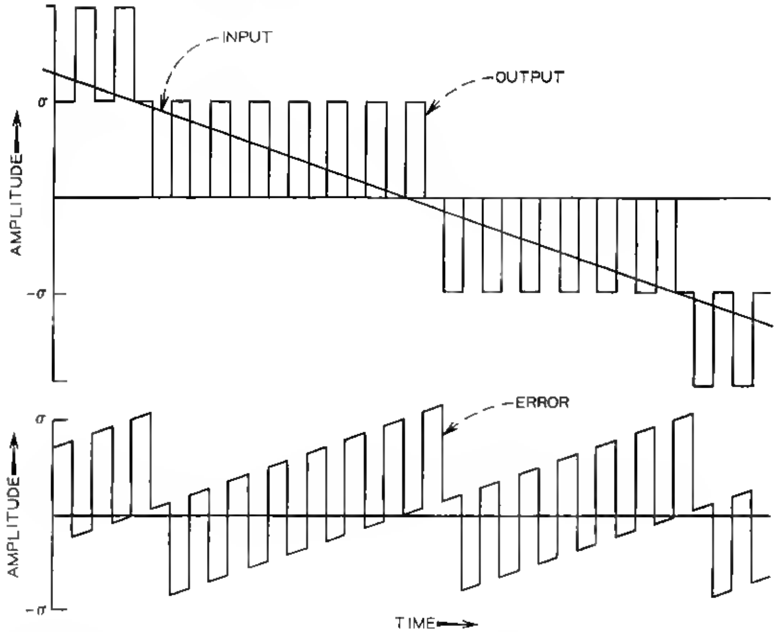

Fig. 6 — Input, output, and error waves for a (negative) ramp input to a symmetrical coder.

Then

$$f_l = Q\left(\frac{l(1-\vartheta)}{2}\right)f_s \,. \tag{22}$$

Ignoring lines outside the Nyquist interval, and combining terms of $+l$ and $-l$,

$$\nu_{0N}(t) = \sum_{l=1}^{\infty} \frac{2\sigma}{\pi l} \sin\,(\pi l\vartheta_0 + 2\pi f_l t). \tag{23}$$

If we now think of the spectrum as one-sided, we have a collection of lines of frequency

$$f = |f_l| \tag{24}$$

and power

$$P_l = \frac{2\sigma^2}{\pi^2 l^2}. \tag{25}$$

These lines will subsequently be referred to as "main lines," "original lines," "carriers," or "l-lines" (2-line, 5-line, and so on).

Figure 8 is an example of the spectrum, bringing out some of the important qualitative features. One can see that the terms for which $l = 2, 4$, and so on, are the components of the sawtooth, of peak-to-peak amplitude σ and fundamental frequency ϑf_s, evident in Fig. 3. If we choose those values of l which equal aN, where a is a positive integer and N is the odd integer nearest $1/\vartheta$, we have the components of another sawtooth of peak-to-peak amplitude $2\sigma/N \approx 2\epsilon$ and fundamental frequency $|1 - N\vartheta| f_s/2$ (Wang's "second envelope function"). In Fig. 8, $N = 19$.

Notice that either the $(N - 2)$-line or the $(N + 2)$-line has a frequency equal to that of the 2-line minus that of the N-line and a power about equal to that of the N-line (the 21-line in Fig. 8). This line may also be thought of as the fundamental of a sawtooth, as may all lines at the lower end of the spectrum.

There is another interesting way of looking at the idle-channel noise spectrum. Recalling equations (15) and (17), it is apparent that $\nu_0(t)$ can be thought of as the result of sampling, at a rate f_s, the wave

$$x_0(t) = \sum_{l \neq 0} \frac{\sigma}{\pi i l} \exp \{\pi i l[\vartheta_0 + (1 - \vartheta) f_s t]\} \tag{26}$$

which describes a sawtooth of peak-to-peak amplitude 2σ and funda-

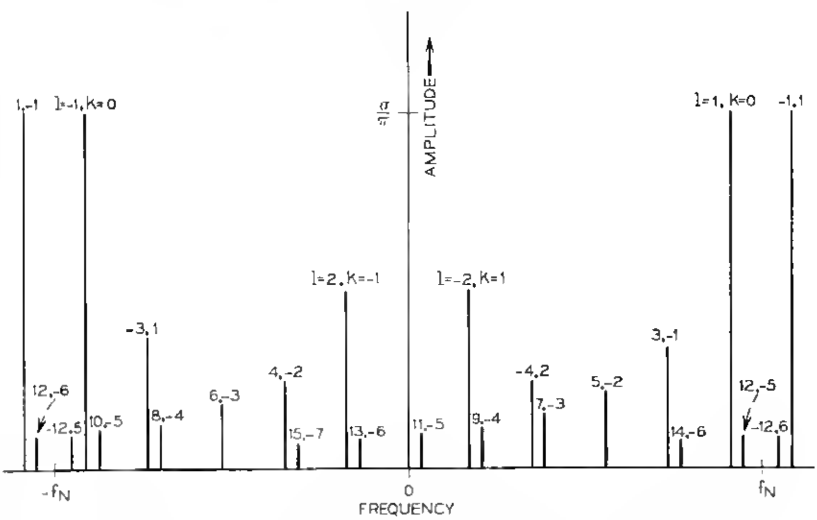

Fig. 7 — Example of an idle-channel noise spectrum. All lines for $|l| = 1, 2, 3, 4$, and 12 are given; notice their symmetries. Selected other lines are included to show the progressions involved.

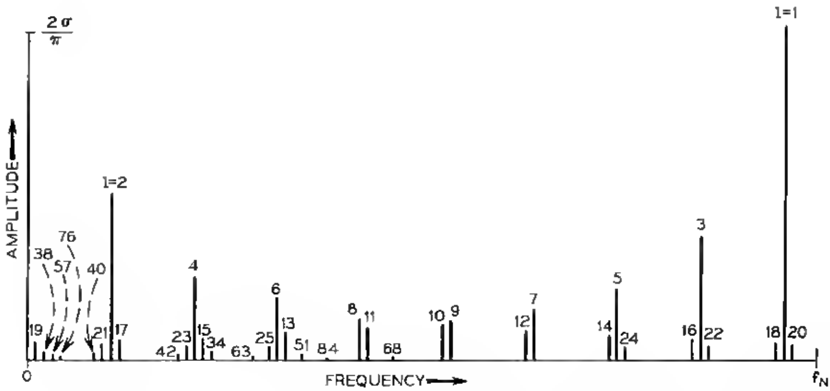

Fig. 8 — Example of a one-sided idle-channel noise spectrum, for $\vartheta = 5/96$. The most powerful 25 lines are shown along with selected others, in particular the harmonics of the 17-line, 19-line, and 21-line. These and the 2-line plus its harmonics make up sawtooth waves.

mental frequency $(1 - \vartheta)f_N$. In Fig. 9 this sawtooth is superimposed on the wave of Fig. 3.

All the l-lines are distinct if ϑ is irrational, which is expected to be the normal case. Appendix B treats rational ϑ.

V. SINUSOIDAL INPUT

Let us calculate the noise output of a $\triangle$M coder for a pure sinusoidal input, setting

$$g(t) = A \sin (2\pi f_0 t + \varphi), \tag{27}$$

where φ is an arbitrary constant phase angle. We put equation (27)

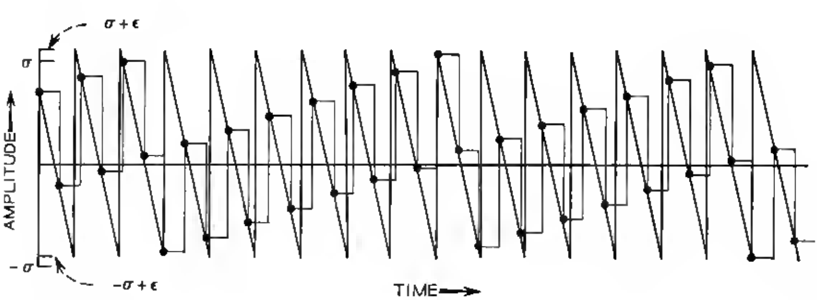

Fig. 9 — Error wave of Fig. 3 with superimposed sawtooth. The heavy dots are the sampling points. Section II explains the vertical offset (ϵ).

into equation (19) and make use of the Jacobi-Anger formula:[6]

$$\exp\left[\pi i l A \sin\left(2\pi f_0 t + \varphi\right)\right] = \sum_{m=-\infty}^{\infty} J_m(\pi l A) \exp\left(2\pi i m f_0 t + i m \varphi\right), \quad (28)$$

where the J_m are the Bessel functions of integral order of the first kind. The result is

$$v_{sin}(t) = \sum_{l \neq 0} \sum_{k=-\infty}^{\infty} \sum_{m=-\infty}^{\infty} \frac{\sigma}{\pi i l} J_m(\pi l A) \cdot \exp\left(\pi i l \vartheta_0 + i m \varphi\right) \exp\left\{2\pi i\left[\left(\frac{l(1-\vartheta)}{2} + k\right) f_s + m f_0\right] t\right\}. \quad (29)$$

If we define

$$f_l' \equiv \left(\frac{l(1-\vartheta)}{2} + k(l, m)\right) f_s , \quad (30)$$

where $k(l, m)$ is chosen so that $f_l' + m f_0$ is in the Nyquist interval, we can write (for this interval)

$$v_{N sin}(t) = \sum_{l=1}^{\infty} \sum_{m=-\infty}^{\infty} \frac{2\sigma}{\pi l} J_m(\pi l A) \sin\left[2\pi(f_l' + m f_0) t + \pi l \vartheta_0 + m \varphi\right]. \quad (31)$$

Equation (31) describes a collection of lines consisting of the original lines of the idle-channel noise spectrum (or their replicas, $f_l + k f_s$), each with a set of uniformly spaced ($\pm m f_0$) satellites. The total power in an l-group (all the lines governed by the index l) is constant. $J_0^2(\pi l A)$ of the power remains in the main line; the mth satellite gets $J_m^2(\pi l A)$ of the total power. From the symmetry of the spectrum one can see that for every l-line satellite which falls outside the Nyquist interval there is a corresponding satellite in the Nyquist interval arising from a carrier outside the interval.

The nature of the Bessel function is such that main lines go through a series of peaks and nulls as a function of A for a given l, and l for a given A. The satellites, in addition, fluctuate in amplitude as a function of the index m. As a result, for the typical case of a signal band which is a small fraction of the Nyquist interval and for an input frequency of the same order as the signal bandwidth, the signal-band noise power is determined by relatively few lines and can be expected to fluctuate irregularly as a function of input amplitude and frequency.

$J_m(z)$ goes fairly rapidly to zero as a function of m for $m > z$. Thus the full width of an l-group is

$$\Delta f \approx 2\pi l A f_0 . \quad (32)$$

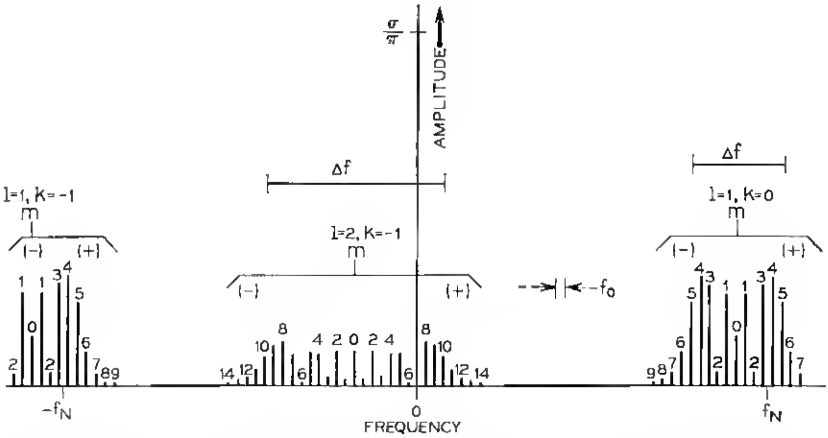

Fig. 10 — The $l = 1$ and $l = 2$ lines of the spectrum of Fig. 7, modulated by a sinusoidal input with $f_0 \approx f_N/40$ and $\pi A = 5$. The other lines are omitted for the sake of clarity. (The lack of symmetry in this figure, and in Fig. 11, is due to the omission of the image groups: $l = -1, -2$.) Equation (32) gives Δf.

Figure 10 gives an example of the spectrum which attempts to bring out the points made above. If f_0 and f_s are not rationally related, the lines are all distinct. Appendix C treats the case of rational f_0/f_s.

VI. BROADBAND INPUT

As first discussed by Bennett, the average noise performance of a coder in the presence of a broadband input signal is best calculated by using an input signal of random phase.[7] This test signal should have the same power spectrum as the input signal under consideration. Appendix D gives the mathematical manipulations.

Briefly the procedure is to calculate the noise power spectrum, $W(f)$, by finding the Fourier transform of the autocorrelation function, $R(\tau)$, of the noise wave. The averaging procedure in the definition of $R(\tau)$ is carried out assuming the input, $g(t)$, is a gaussian variate. This gives $R(\tau)$ in terms of the autocorrelation coefficients, a_k, and the mean power of the sequence of input samples; we determine the a_k from the Fourier transform of the input power spectrum, $U(f)$. We show that, under an assumption that usually holds in practice, the dependence on $U(f)$ reduces to a dependence on the rms time derivative of the input. A parameter S, which is this time derivative normalized to the average maximum slope of the coder, σf_s, characterizes the input in the following (equivalent) formulas:

$$W(f) = \sum_{l \neq 0} \sum_{k=-\infty}^{\infty} \frac{\tau_s \sigma^2}{\pi^2 l^2} \exp\left[-\frac{(\pi l k S)^2}{2} + 2\pi i k\left(f\tau_s + \frac{l(1-\vartheta)}{2}\right)\right], \quad (33)$$

$$W(f) = \sum_{l \neq 0} \sum_{p=-\infty}^{\infty} \frac{2^{1/2}\tau_s \sigma^2}{\pi^{5/2} \mid l \mid^3 S} \exp\left[-\frac{2}{(lS)^2}\left(f\tau_s + \frac{l(1-\vartheta)}{2} + p\right)^2\right]. \quad (34)$$

Terms of different l do not interact in equations (33) and (34); therefore, one may use either formula to calculate the power density for a given l. Equation (33) converges faster for high values of l; equation (34) for low values. The crossover occurs at $l \approx 1/(\pi)^{\frac{1}{2}}S$.

One can see [most easily from (34)] that the spectrum consists of the lines given in Section IV for the idle-channel noise spectrum, each now broadened to a gaussian. Notice that some of the power in the wings of each gaussian falls outside $(-f_N, f_N)$. Conversely, lines centered outside this band have in-band wings. The total in-band power of each l-group is constant.

One can easily see that the full width of an l-group is

$$\Delta f = lSf_s. \quad (35)$$

Thus for $lS \ll 1$ one has a relatively sharp line, while all groups for which $lS \gtrsim 1$ sum to a white background. Figure 11 shows the important qualitative features of the spectrum.

As S approaches one, equations (33) and (34) lose their usefulness because of the onset of so-called slope-overload noise. (Strictly speaking equations (8) and (9) do not apply under overload conditions; but because the errors resulting from overload and quantization are prob-

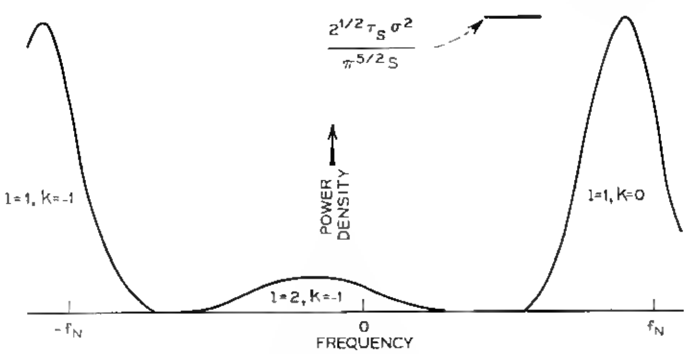

Fig. 11 — The $l = 1$ and $l = 2$ lines of the spectrum of Fig. 7, modulated by a gaussian input with $S \approx 1/8$. The other lines are omitted for the sake of clarity.

ably largely uncorrelated, one should be able to calculate them separately with reasonable precision.) To give some idea of the effect, we quote Protonotarios' signal-to-overload-noise ratios for various input spectra: 3 to 17 dB for $S = 1$ and 16 to 31 dB for $S = \frac{1}{2}$.[8] These values are lower limits, and probably poor approximations for high-quality voice systems, because the total noise was used. Nevertheless, it seems safe to say that the occurrence of slope overload will prohibit inputs strong enough to whiten the 1-group and, usually, the 2-group as well.

Figure 12 illustrates calculated noise spectra of a coder suitable for telephone applications.[1] Notice the enormous differences in power in the voice band for different ϑ's. For $\vartheta = 0.02$ the 2-line, 4-line, and 6-line centered at 30.88, 61.76, and 92.64 kHz, respectively, can be seen. The broad line centered at 38.6 kHz for $\vartheta = 0.05$ and $S = 2^{-10}$ is the sum of the 19- and 21-lines. Although the spectra are white for $S = 2^{-2}$ in the frequency range shown, they are not independent of S. The 2-line is still spreading out and the 1-line is just starting to spread in.

Figure 13 presents the results of Fig. 12 in the form of noise power in dBrnC versus speech input power in dBm. The unit "dBrnC" means dB above one picowatt of integrated noise passing through a filter with C-message weighting.[9] Briefly, this filter, which weights noise according to its subjective effect in a telephone circuit, has a pass band with a transmission averaging about -0.5 dB from ≈ 800 to ≈ 2500 Hz; the noise bandwidth is ≈ 2070 Hz.

The parameter S is turned into speech power as follows: de Jager (see p. 447 of Ref. 2) showed that the ratio of the rms slope of the average speech spectrum[10] to the rms amplitude is given by

$$r \equiv \left(\frac{\langle \dot{y}^2 \rangle}{\langle y^2 \rangle}\right)^{\frac{1}{2}} \approx 2\pi \cdot 800 \text{ Hz} \approx 5000 \text{ rad per s}. \tag{36}$$

Thus, speech power is given by

$$P_{sp} = \left(\frac{S\sigma f_s}{r}\right)^2. \tag{37}$$

In Fig. 13, this quantity is plotted in units of dB above 1 mW. The structure in Fig. 13 is best interpreted by referring to Fig. 12.

VII. SUMMARY AND REMARKS

We have developed a ΔM quantizing-noise formalism for the case of unequal positive and negative integrator step sizes and have given the noise spectrum for zero, sinusoidal, and gaussian coder inputs.

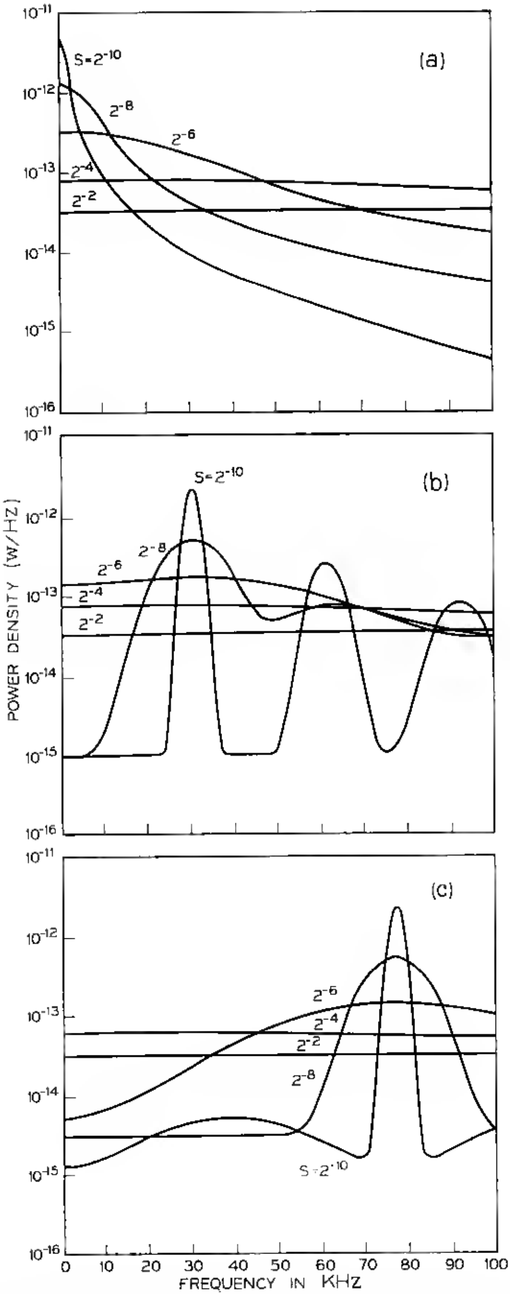

Fig. 12 — Partial one-sided noise spectra for gaussian inputs with $\sigma = 0.4$ mV/$\Omega^{1/2}$ (12-mV steps in 900Ω), $f_s = 1.544$ MHz, and various values of ϑ and S. (a) $\vartheta = 0$, (b) $\vartheta = 0.02$, and (c) $\vartheta = 0.05$.

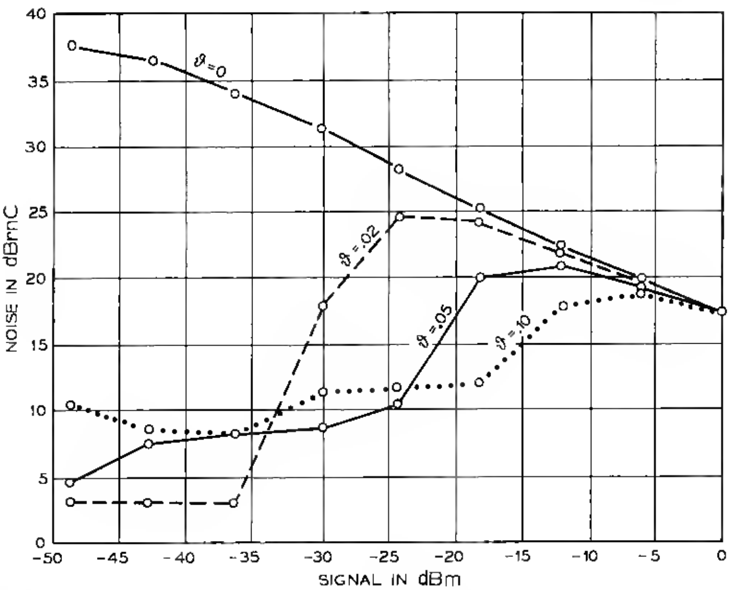

Fig. 13 — Noise versus average speech power for the coder of Fig. 12. See text for explanation of units. The circles are the calculated points; the lines are only to connect points of the same parameter.

In ΔM systems, as contrasted with multibit PCM and DPCM, the signal typically does not change more than a small fraction of a step size in one sampling interval. As a result, the sample-to-sample errors are strongly correlated and the noise spectrum is highly colored. The main contributions of this paper are to point out that the spectral distribution of power is strongly dependent on the step unbalance and to provide a means of calculating the spectrum precisely.

A typical ΔM system has a signal handwidth very much smaller than the Nyquist handwidth. The consequences of this situation for the idle channel (zero input) are best seen hy referring to Figs. 7 and 8. There are extreme system-noise variations depending on whether or not the system parameters are such as to bring into the signal band one of the stronger spectral lines. The $| l | = 2$-line, which has $\approx$15 percent of the total Nyquist-interval power, is especially important in this regard.

Coder inputs phase-modulate the idle-channel lines; the frequency breadth of the sideband structure is proportional to the rms slope (roughly, root power times frequency) of the input. Thus, as power is

increased, there may be an abrupt increase in noise as the sidebands of a strong line come into the signal band. Figure 13 illustrates such a situation.

At very high input powers most of the idle-channel lines are broadened to the point where they make an easily calculable white contribution to the spectrum. Unfortunately, the most powerful lines ($|l| = 1$ with 61 percent of the Nyquist-interval power, $|l| = 2$, and so on) can be broadened to whiteness only by inputs powerful enough to force the coder into slope overload. It is possible, however, to minimize noise in a given system by dithering, that is, the deliberate injection of certain appropriate signals into the coder (including the judicious choice of step unbalance). Dithering requires extensive treatment and will be the subject of a future paper.

VIII. ACKNOWLEDGMENT

I thank D. J. Goodman for a critical reading of the manuscript.

APPENDIX A

Correlation of Error and Input

The error wave, $\nu(t)$, consists in general of a part fully correlated with the input, $g(t)$, and an uncorrelated part. The uncorrelated part is noise in almost any conceivable system; whether the fully correlated part is considered noise or not depends on the use to which the system is put. Let us investigate the correlation by forming the cross-correlation function of ν and g (assuming zero mean for each):

$$R_{\nu g}(\tau) \equiv \lim_{T\to\infty} \frac{1}{2T} \int_{-T}^{T} \nu(t) g(t + \tau)\, dt. \tag{38}$$

Inserting equation (19) gives

$$R_{\nu g}(\tau) = \sum_{l\neq 0} \frac{\sigma}{\pi i l} \exp(\pi i l \vartheta_0) \lim_{T\to\infty} \frac{1}{2T} \cdot \int_{-T}^{T} g(t + \tau) e^{\pi i l g(t)} \sum_{k=-\infty}^{\infty} \exp\left[2\pi i\left(\frac{l(1-\vartheta)}{2} + k\right) f_s t\right] dt. \tag{39}$$

The integral in equation (39) is zero unless $g(t)$ contains components locked to the idle-channel-noise frequencies (Section IV) or their subharmonics. Thus for typical ΔM systems

$$R_{\nu g}(\tau) = 0 \quad \text{for all} \quad \tau, \tag{40}$$

and $\nu(t)$ is a noise wave under any circumstances.

This conclusion is not applicable to the case of rational ϑ, treated in Appendix B, where $l(1 - \vartheta)/2 + k = 0$ for some values of l and k; that is, some of the idle-channel-noise frequencies are zero. The most extreme case is that of PCM ($\vartheta = 1$) where every value of l contributes a dc term to the summation in equation (39) and the summation is therefore replaced by one. Let us calculate the two parts of $\nu(t)$ for this case.

It is easy to show that $R_{\nu g}(\tau)$ is a maximum for $\tau = 0$ and that we need consider only instantaneous correlations. This result is physically reasonable when one considers that no delay from input to output was introduced in the formulation of $\nu(t)$. If we let $\langle \quad \rangle_{av}$ stand for the integrating-limiting (averaging) process defined in equation (38) we can write

$$\langle \nu g \rangle_{av} \equiv R_{\nu g}(0). \tag{41}$$

The correlated part of $\nu(t)$ is $\alpha y(t)$, where α is a constant for a given $y(t)$. The uncorrelated part is then $\nu(t) - \alpha y(t)$, and the condition for determining α is

$$\langle (\nu - \alpha y) y \rangle_{av} = 0, \tag{42}$$

or

$$\alpha = \frac{\langle \nu y \rangle_{av}}{\langle y^2 \rangle_{av}} = \frac{\langle \nu g \rangle_{av}}{\sigma \langle g^2 \rangle_{av}}. \tag{43}$$

Substitution of a specific input waveform into

$$\langle \nu g \rangle_{av} = \sum_{l \neq 0} \frac{\sigma}{\pi i l} \exp(\pi i l \vartheta_0) \langle g(t) e^{\pi i l g(t)} \rangle_{av} \tag{44}$$

will show that αy is generally negligible compared with ν unless $\langle g^2 \rangle_{av} < 1$; that is, the signal-to-noise ratio is low. This conclusion is quite plausible because of the $\langle g^2 \rangle^{-1}$ dependence of α and because the oscillatory character of the second factor in the averaging bracket in equation (44) makes the bracket tend toward zero as g increases.

For rational values of $\vartheta \neq 1$, the summation in equation (44) is only over multiples of an integer L (as shown in Appendix B) and αy is negligible for even smaller values of $\langle g^2 \rangle$. $L = 2$ for the van de Weg case, $\vartheta = 0$.

APPENDIX B

Rational Step Unbalance

If the fractional step unbalance, ϑ, is a rational number, the l-lines of Section IV are not all distinct. Indeed, if L is the least positive integer for which $(L/2)(1 - \vartheta)$ is an integer, it is easy to see from equation (22) that

$$f_{l+L} = f_l \quad \text{and} \quad f_{L-l} = -f_l \,. \tag{45}$$

Let us sum up terms of frequency $\pm f_l$ in equation (23), ignoring for the moment the cases $l = L$ and $l = L/2$ (if it exists). Then

$$\nu_{ONl}(t) = \sum_{l'=0}^{\infty} \frac{2\sigma}{\pi(l + l'L)} \sin\,[\pi(l + l'L)\vartheta_0 + 2\pi f_l t]$$
$$+ \sum_{l'=0}^{\infty} \frac{2\sigma}{\pi(L - l + l'L)} \sin\,[\pi(L - l + l'L) - 2\pi f_l t]. \tag{46}$$

A little manipulation of the indices in the second summation gives

$$\nu_{ONl}(t) = \sum_{l'=-\infty}^{\infty} \frac{2\sigma}{\pi(l + l'L)} \sin\,[\pi(l + l'L)\vartheta_0 + 2\pi f_l t] \tag{47}$$

$$= \sum_{l'=-\infty}^{\infty} \frac{\sigma}{\pi i(l + l'L)} \exp\,\{i[\pi(l + l'L)\vartheta_0 + 2\pi f_l t]\} + \text{c.c.*}. \tag{48}$$

From Jolley's series Nos. 534 and 535 it is easily established that[11]

$$\sum_{n=-\infty}^{\infty} \frac{e^{in\psi}}{a + n} = \pi \csc a\pi e^{ia(\pi - \psi)} \quad \text{for} \quad 0 < \psi < 2\pi. \tag{49}$$

Using this to do the sum in equation (48),

$$\nu_{ONl}(t) = \frac{\sigma \csc\left(\frac{l}{L}\pi\right)}{iL} \exp\left[i\left(\frac{l}{L}\pi - \pi l\vartheta_1 + \pi l\vartheta_0 + 2\pi f_l t\right)\right] + \text{c.c.} \tag{50}$$

$$= \frac{2\sigma \csc\left(\frac{l}{L}\pi\right)}{L} \sin\left(\pi\frac{l}{L} - \pi l\vartheta_1 + \pi l\vartheta_0 + 2\pi f_l t\right), \tag{51}$$

where

$$L\vartheta_1 = \text{least positive quantity} \equiv L\vartheta_0 \bmod 2. \tag{52}$$

---

* By c.c. we mean complex conjugate.

The power at $f = | f_l |$ is thus

$$P_l = \frac{2\sigma^2 \csc^2 \left(\frac{l}{L}\pi\right)}{L^2}. \tag{53}$$

Let us compare this with the sum of the powers of the same lines as given by equation (25):

$$P_l' = \sum_{l'=0}^{\infty} \left(\frac{2\sigma^2}{\pi^2 (l + l'L)^2} + \frac{2\sigma^2}{\pi^2 (L - l + l'L)^2} \right). \tag{54}$$

Again, index manipulation yields

$$P_l' = \sum_{l'=-\infty}^{\infty} \frac{2\sigma^2}{\pi^2 (l + l'L)^2}. \tag{55}$$

This series is easily summed by means of cotangent residues (see Section 7.4-4 of Ref. 6) to give

$$P_l' = \frac{2\sigma^2 \csc^2 \left(\frac{l}{L}\pi\right)}{L^2}, \tag{56}$$

which is identical to equation (53). Thus, all lines with the same frequency, f, where $0 < f < f_N$, are phased such that their powers add. As a result one need not take line degeneracies into special account when considering the noise power spectrum. We assume, without proof, that this statement is true of sidebands as well as main lines; it is elementary that the power in a sine wave is not changed when its phase is modulated.

If L is even there is a line at $f_{L/2} = f_N$, on the border between the Nyquist interval and higher frequencies. If one starts from equation (20) rather than equation (23), so that the higher frequencies are taken into account, equation (51) with $l = L/2$ will result.

For $l = l' L$ we get $f_l = 0$, that is, a dc component. Summing up these terms of equation (23),

$$\nu_{ONL}(t) = \sum_{l'=1}^{\infty} \frac{2\sigma}{\pi l' L} \sin \pi l' L \vartheta_0 . \tag{57}$$

Starting from equation (49), subtracting the $n = 0$ term $(1/a)$ from both sides, letting $a \to 0$, and combining terms of $+n$ and $-n$, gives

$$\sum_{n=1}^{\infty} \frac{\sin n\psi}{n} = \frac{\pi - \psi}{2} \quad \text{for} \quad 0 < \psi < 2\pi. \tag{58}$$

Using equation (58) in equation (57) gives

$$\nu_{0NL} = \frac{\sigma}{L}(1 - L\vartheta_1), \tag{59}$$

where ϑ_1 is defined in equation (52). Thus, the dc component fluctuates as a function of ϑ_1 or ϑ_0. If it is averaged uniformly over this parameter, the mean value is zero and the mean square is $\sigma^2/3L^2$. The latter is the sum of the powers of the $l'L$-lines. The dc power varies from zero to σ^2/L^2. Thus, for rational ϑ, the total noise power in the Nyquist interval (counting one-half the power at f_N) is not always $\sigma^2/3$ but can vary from this total by $-\sigma^2/3L^2$, $+2\sigma^2/3L^2$. For small ϑ and correspondingly large L this variation is not very significant. In any case, as Section III explains, the usual ΔM system suppresses dc at the decoder.

If the $l'L$-lines are modulated, we have

$$\nu_{NL}(t) = \sum_{l'=1}^{\infty} \frac{2\sigma}{\pi l'L} \sin \pi l'L[\vartheta_0 + g(t)] \tag{60}$$

$$= \frac{\sigma}{L}[1 - L\vartheta_1(t)], \tag{61}$$

where $\vartheta_1(t)$ is defined by using $\vartheta_0 + g(t)$ in equation (52) in place of ϑ_0. If the excursions of $g(t)$ are significantly greater than $1/L$ ($\langle g^2 \rangle \gg 1/L^2$, which covers nearly all cases of practical interest) equation (61) can be time-averaged uniformly over $\vartheta_1(t)$. As stated above, the mean square will be $\sigma^2/3L^2$. That is, for a practical input signal, the power in the $l'L$-lines is dispersed into sidebands, and the total power in these sidebands is equal to that which would be calculated using the formulas for irrational ϑ. This argument is used to justify the assumption that, except for dc power, the noise spectrum for rational ϑ can be calculated as indicated in the text for irrational ϑ.

There are two cases of rational ϑ which are of special interest. One is $\vartheta = 0$, calculated for gaussian input by van de Weg[3]. In this case all the even-l lines are centered at zero frequency and all the odd-l lines at f_N. As one can see from Section VI and Figs. 12 and 13, this is a good approximation only for a baseband with a width much greater than ϑf_s.

The other case of interest is $\vartheta = 1$. This is equivalent to using the even-instant law of equation (8) for all sampling instants, which is equivalent to ordinary uniform PCM (with a step size of 2σ). Let us consider a typical PCM speech system, for which (see Section VI)

$$\langle \dot{g}^2 \rangle = \langle g^2 \rangle \cdot (2\pi \cdot 800 \text{ Hz})^2 \tag{62}$$

and

$$f_s = 8 \text{ kHz}. \tag{63}$$

Then (Appendix D)

$$S \approx 0.63\langle g^2 \rangle^{\frac{1}{2}}. \tag{64}$$

Useful input signals are many steps high in amplitude ($\langle g^2 \rangle \gg 1$); thus $S > 1$ and the noise spectrum is substantially white. (See Section VI. This range of S is permissible for PCM, since slope overload does not occur.)

If $\vartheta = 1$ is inserted into equation (31) the result can be shown to be equivalent to that of Schouten and van't Groenewout for a sinusoidal input into a PCM coder if one allows for:[12] (*i*) their nonunity shape factor, (*ii*) their particular choice of phase (φ), (*iii*) replacing the last sine factor in their expression (17) by a cosine, and (*iv*) multiplying their expressions (15), (16), and (17) by 2.

APPENDIX C

Rational Input-to-Sampling Frequency Ratio

If the ratio of f_0 to f_s is a rational fraction, there exists a least positive integer M for which Mf_0/f_s is integral. In this case it is easily seen, from equation (29), that terms for which the values of m differ by a multiple of M have the same Nyquist-interval frequency. Summing up these equal-frequency terms, we replace equation (29) with

$$\nu_{\sin}(t) = \sum_{l \neq 0} \sum_{k=-\infty}^{\infty} \sum_{m=1}^{M} \frac{\sigma}{\pi i l} \sum_{m'=-\infty}^{\infty} J_{m+m'M}(\pi l A) \exp\left[i(m + m'M)\varphi\right]$$
$$\cdot \exp\left\{\pi i l \vartheta_0 + 2\pi i\left[\left(\frac{l(1-\vartheta)}{2} + k\right)f_s + mf_0\right]t\right\}. \tag{65}$$

One can therefore see that a given l-group consists of a total of M lines, the original and $M-1$ satellites spaced uniformly throughout $(-f_N, f_N)$.

The sum over m' in equation (65), which is the relative amplitude coefficient of a satellite $[B_m(z, \varphi, M)$, where $z = \pi l A]$ can be turned into a finite sum:

It is easy to verify that

$$\frac{1}{M} \sum_{n=1}^{M} \exp\left(\frac{2\pi i n(m-p)}{M}\right) = 1 \quad \text{if} \quad p = m + m'M$$
$$= 0 \quad \text{otherwise}, \tag{66}$$

where m, m', M, and p are integers.

Thus

$$B_m(z, \varphi, M) \equiv \sum_{m'=-\infty}^{\infty} J_{m+m'M}(z) \exp\,[i(m + m'M)\varphi] \tag{67}$$

$$= \sum_{p=-\infty}^{\infty} J_p(z) e^{ip\varphi} \left[\frac{1}{M} \sum_{n=1}^{M} \exp\left(\frac{2\pi i n(m-p)}{M} \right) \right] \tag{68}$$

$$= \frac{1}{M} \sum_{n=1}^{M} \sum_{p=-\infty}^{\infty} J_p(z) \exp\left[ip\left(\varphi - \frac{2\pi n}{M}\right)\right] \exp\left(\frac{2\pi i n m}{M}\right). \tag{69}$$

The sum over p is given by equation (28). Thus

$$B_m(z, \varphi, M) = \frac{1}{M} \sum_{n=1}^{M} \exp\left[iz \sin\left(\varphi - \frac{2\pi n}{M}\right) + \frac{2\pi i n m}{M}\right]. \tag{70}$$

We note the dependence on the phase (φ) of the input signal, which indicates that this result could not have been obtained by adding the powers of the equal-frequency terms. Indeed, it can be established easily from equation (67) that

$$\frac{1}{2\pi} \int_0^{2\pi} |\, B_m(z, \varphi, M) \,|^2 \, d\varphi = \sum_{m'=-\infty}^{\infty} J^2_{m+m'M}(z); \tag{71}$$

that is, the sum of the term powers is given by the true satellite power averaged uniformly over φ.

In order to emphasize this dependence on phase, let us examine the highly artificial but simplest nontrivial case, $f_0 = f_N$. In this case $M = 2$ and each main line has one satellite spaced f_N away. Then

$$B_0(z, \varphi, 2) = B_2(z, \varphi, 2) = \cos\,(z \sin \varphi), \tag{72}$$

and

$$B_1(z, \varphi, 2) = i \sin\,(z \sin \varphi). \tag{73}$$

For $\varphi = 0$, the satellite power is always zero and we get the undisturbed idle-channel-noise spectrum. That this is to be expected can be seen from equation (27) where $\varphi = 0$ is the condition under which the sampling instants fall precisely on the zeroes of the input wave. For $\varphi = \pi/2$, where the sampling instants fall on the crests, the power for any given l oscillates between main and satellite as a function of amplitude. This result may be compared with the incorrect one obtained by summing powers:

$$\frac{1}{2\pi} \int_0^{2\pi} |\, B_0(z, \varphi, 2) \,|^2 \, d\varphi = \frac{1 + J_0(2z)}{2}, \tag{74}$$

and

$$\frac{1}{2\pi}\int_0^{\pi} |B_1(z,\varphi,2)|^2\,d\varphi = \frac{1-J_0(2z)}{2}. \tag{75}$$

APPENDIX D

Calculations for Broadband Input

The autocorrelation function of $\nu(t)$ [defined in equation (14)] is given by

$$R(\tau) = \lim_{T\to\infty}\frac{1}{2T}\int_{-T}^{T}\left(\sum_{n=-\infty}^{\infty} x_n\tau_s\,\delta(t-n\tau_s)\right)$$

$$\cdot\left(\sum_{m=-\infty}^{\infty} x_m\tau_s\,\delta(t-m\tau_s+\tau)\right)dt \tag{76}$$

$$= \lim_{T\to\infty}\frac{\tau_s^2}{2T}\sum_{n\geq -T/\tau_s}^{\leq T/\tau_s}\;\sum_{m\geq(-T+\tau)/\tau_s}^{\leq(T+\tau)/\tau_s} x_n x_m\,\delta[\tau+(n-m)\tau_s]. \tag{77}$$

We can replace T/τ_s with a positive integer N without loss of generality. Let us concentrate on values of τ lying between $(k-1/2)\tau_s$ and $(k+1/2)\tau_s$ where k is an integer. Only terms for which $n-m=-k$ fall within this interval. Thus

$$R(\tau) = \tau_s\lim_{N\to\infty}\frac{1}{2N}\sum_{n=-N}^{N} x_n x_{n+k}\,\delta(\tau-k\tau_s)$$

$$\text{for}\quad (k-\tfrac{1}{2})\tau_s < \tau \leqq (k+\tfrac{1}{2})\tau_s\,. \tag{78}$$

Defining

$$\langle x_n x_{n+k}\rangle \equiv \lim_{N\to\infty}\frac{1}{2N}\sum_{n=-N}^{N} x_n x_{n+k}\,, \tag{79}$$

and joining together the segments of the function given by equation (78), we have

$$R(\tau) = \tau_s\sum_{k=-\infty}^{\infty}\langle x_n x_{n+k}\rangle\,\delta(\tau-k\tau_s). \tag{80}$$

The Fourier transform of $R(\tau)$ is the noise-power spectral density, first given by Bennett (see pp. 460–464 of Ref. 7):

$$W(f) = \tau_s\sum_{k=-\infty}^{\infty}\langle x_n x_{n+k}\rangle\exp(2\pi ikf\tau_s). \tag{81}$$

It is easy to see that

$$\int_{-f_N}^{f_N} W(f)\, df = \langle x_n x_n \rangle \equiv \langle x^2 \rangle; \tag{82}$$

that is, the total noise power in the Nyquist interval is given by the mean square of the sequence $\{x_n\}$.

Next, let us connect $\langle x_n x_{n+k} \rangle$ with the input signal. Using equation (12)

$$\langle x_n x_{n+k} \rangle = \Big\langle \sum_{l \neq 0} \sum_{\lambda \neq 0} - \frac{\sigma^2}{\pi^2 l \lambda}$$
$$\cdot \exp \{\pi i[(l + \lambda)\vartheta_0 + (l + \lambda)n(1 - \vartheta) + lk(1 - \vartheta) + lg_{n+k} + \lambda g_n]\} \Big\rangle. \tag{83}$$

We carry the averaging bracket inside the summations and examine the various factors of the exponential. Since n and g_n are uncorrelated, the factors containing them can be averaged separately. Let us examine the factor

$$\langle e^{\pi i (l+\lambda) n (1-\vartheta)} \rangle.$$

For irrational ϑ this expression is zero unless $l + \lambda = 0$, in which case its value is one. Thus equation (83) reduces to

$$\langle x_n x_{n+k} \rangle = \sum_{l \neq 0} \frac{\sigma^2}{\pi^2 l^2} e^{\pi i l k (1-\vartheta)} \langle \exp [\pi i l (g_{n+k} - g_n)] \rangle. \tag{84}$$

Notice that (see p. 66 of Ref. 12)

$$\langle x^2 \rangle = \sum_{l \neq 0} \frac{\sigma^2}{\pi^2 l^2} = \frac{\sigma^2}{3}. \tag{85}$$

Let us now find the value of the averaging bracket in equation (84) for a gaussian input:

$$\langle \exp [\pi i l (g_{n+k} - g_n)] \rangle$$
$$= \int_{-\infty}^{\infty} \int_{-\infty}^{\infty} \exp [\pi i l (g_{n+k} - g_n)] P(g_{n+k}\, , g_n)\, dg_{n+k}\, dg_n\, , \tag{86}$$

where $P(g_{n+k}, g_n)$ is the joint probability density of two gaussian variates, which is (see Section 18.8–6 of Ref. 6):

$$P(g_{n+k}\, , g_n) = \frac{1}{2\pi \langle g^2 \rangle (1 - a_k^2)^{\frac{1}{2}}} \cdot \exp \left(- \frac{g_n^2 - 2a_k g_n g_{n+k} + g_{n+k}^2}{2\langle g^2 \rangle (1 - a_k^2)} \right), \tag{87}$$

where

$$a_k = \frac{\langle g_n g_{n+k} \rangle}{\langle g^2 \rangle}, \tag{88}$$

$$\langle g_n g_{n+k} \rangle \equiv \lim_{N \to 0} \frac{1}{2N} \sum_{m=-N}^{N} g_n g_{n+k}, \tag{89}$$

and

$$\langle g^2 \rangle \equiv \langle g_n g_n \rangle. \tag{90}$$

Combining equations (86) and (87) gives

$$\langle \exp [\pi i l (g_{n+k} - g_n)] \rangle = \exp [-\pi^2 l^2 \langle g^2 \rangle (1 - a_k)], \tag{91}$$

a result first obtained by Rice.[13] Substituting equation (91) into equation (84), and the result into equation (81), gives

$$W(f) = \sum_{l \neq 0} \sum_{k=-\infty}^{\infty} \frac{\tau_s \sigma^2}{\pi^2 l^2} \cdot \exp \left[-\pi^2 l^2 \langle g^2 \rangle (1 - a_k) + 2\pi i k \left(f\tau_s + \frac{l(1 - \vartheta)}{2} \right) \right]. \tag{92}$$

This result, with $\vartheta = 0$, was given by van de Weg.[3] He also used as an input a flat signal, band-limited to $(-f_m, f_m)$, for which

$$a_k = \frac{\sin (2\pi k f_m \tau_s)}{2\pi k f_m \tau_s}, \tag{93}$$

and inserted

$$1 - a_k \approx \frac{(2\pi k f_m \tau_s)^2}{6}. \tag{94}$$

This approximation is made possible by observing that the real exponential factor in equation (92) is appreciable only for small values of the exponent. Thus, if one ignores the region of low signal-to-noise ratios (that is, small $\langle g^2 \rangle$), $1 - a_k$ need only be accurately approximated for small values. $\langle g^2 \rangle > 0.1$ is high enough for the approximation to be good for most purposes, and appears to cover nearly all cases of practical interest.

It is not necessary for the input spectrum to be flat. We take a spectrum, $U(f)$, even in f and confined to the Nyquist interval. Appendix E shows that $\langle g_n g_{n+k} \rangle$ is given by $R_g(k\tau_s)$, the autocorrelation function of $g(t)$. This autocorrelation function is the Fourier trans-

form of the spectral density.

$$\langle g_n g_{n+k} \rangle = \int_{-\infty}^{\infty} U(f) \exp (2\pi i k f \tau_s) \, df \tag{95}$$

and [using the evenness of $U(f)$]

$$\langle g^2 \rangle (1 - a_k) = \int_{-\infty}^{\infty} U(f)(1 - \cos 2\pi k f \tau_s) \, df. \tag{96}$$

Using the reasoning given in the previous paragraph, and specifying that $U(f)$ be a smooth function of frequency (free of strong narrow-band components which could make $1 - a_k \approx 0$ for isolated high values of k), gives

$$\langle g^2 \rangle (1 - a_k) \approx \frac{k^2}{2f_s^2} \int_{-\infty}^{\infty} (2\pi f)^2 U(f) \, df. \tag{97}$$

It is well known that the integral in equation (97) gives the mean square of the time derivative of $g(\equiv \dot{g})$. Thus

$$\langle g^2 \rangle (1 - a_k) \approx \frac{k^2 \langle \dot{g}^2 \rangle}{2f_s^2} = \frac{k^2 \langle \dot{y}^2 \rangle}{2\sigma^2 f_s^2} \equiv \frac{k^2 S^2}{2}, \tag{98}$$

where S is the rms time slope of the input normalized to the maximum average slope of the coder (σf_s). Inserting equation (98) into equation (92) gives

$$W(f) = \sum_{l \neq 0} \sum_{k=-\infty}^{\infty} \frac{\tau_s \sigma^2}{\pi^2 l^2} \exp \left[-\frac{(\pi l k S)^2}{2} + 2\pi i k \left(f \tau_s + \frac{l(1 - \vartheta)}{2} \right) \right] \tag{99}$$

which is equation (33).

Making use of the Fourier-series expansion of a picket fence of gaussians,

$$\sum_{p=-\infty}^{\infty} \exp [-\alpha^2 (x - p x_0)^2] = \sum_{k=-\infty}^{\infty} \frac{\pi^{\frac{1}{2}}}{|\alpha| x_0} \exp \left[-\left(\frac{\pi k}{\alpha x_0} \right)^2 + \frac{2\pi i k x}{x_0} \right], \tag{100}$$

we can rewrite equation (99) as

$$W(f) = \sum_{l \neq 0} \sum_{p=-\infty}^{\infty} \frac{2^{1/2} \tau_s \sigma^2}{\pi^{5/2} |l|^3 S} \exp \left[-\frac{2}{(lS)^2} \left(f \tau_s + \frac{l(1 - \vartheta)}{2} + p \right)^2 \right] \tag{101}$$

which is equation (34).

Computationally more convenient versions of equations (99) and (101) are, in one-sided form,

$$P(f) = \frac{8\tau_s\sigma^2}{\pi^2} \cdot \left\{ \sum_{l=1}^{\infty} \frac{1}{l^2} \left[\frac{1}{2} + \sum_{k=1}^{\infty} \exp\left(-\frac{(\pi l k S)^2}{2} \right) \cos \pi l k(1 - \vartheta) \cos 2\pi k f \tau_s \right] \right\}, \tag{102}$$

and

$$P(f) = \frac{2^{3/2}\tau_s\sigma^2}{\pi^{5/2} S} \sum_{l=1}^{\infty} \left(\frac{1}{|\,l\,|^3} \sum_{p=-\infty}^{\infty} \left\{ \exp\left[-\frac{2}{(lS)^2} \left(f\tau_s + p + \frac{l(1-\vartheta)}{2} \right)^2 \right] + \exp\left[-\frac{2}{(lS)^2} \left(f\tau_s + p - \frac{l(1-\vartheta)}{2} \right)^2 \right] \right\} \right). \tag{103}$$

In equation (102), $1/2\ \Sigma(1/l^2)$ is left in that form in order that the power density can be calculated separately for each l.

APPENDIX E

Autocorrelation—Function and Its Samples

In the absence of aliasing, the autocorrelation coefficients of a sequence of samples of a function are equal to the appropriate samples of the autocorrelation of the function:

$$\langle g_n g_{n+k} \rangle = \lim_{N\to\infty} \frac{1}{2N} \sum_{n=-N}^{N} g_n g_{n+k} \tag{104}$$

$$= \lim_{N\to\infty} \frac{1}{2N} \int_{-N\tau_s}^{N\tau_s} \sum_{n=-\infty}^{\infty} g(n\tau_s) g(n\tau_s + k\tau_s)\ \delta(t - n\tau_s)\ dt \tag{105}$$

$$= \lim_{N\to\infty} \frac{1}{2N} \int_{-N\tau_s}^{N\tau_s} g(t) g(t + k\tau_s) \sum_{n=-\infty}^{\infty} \delta(t - n\tau_s)\ dt \tag{106}$$

$$= \lim_{N\to\infty} \frac{1}{2N\tau_s} \int_{-N\tau_s}^{N\tau_s} g(t) g(t + k\tau_s) \sum_{p=-\infty}^{\infty} \exp\ (2\pi i p f_s t)\ dt \tag{107}$$

$$= \lim_{T\to\infty} \frac{1}{2T} \int_{-T}^{T} g(t) g(t + k\tau_s)\ dt \tag{108}$$

$$\equiv R_g(k\tau_s) \tag{109}$$

where the transition from equation (107) to equation (108) is made by assuming that $g(t)$ is confined to the Nyquist interval. For any given

value of $p \neq 0$, equation (107) can be regarded as the correlation function of $g(t)$ and $g(t) \exp(2\pi i p f_s t)$. The latter represents a carrier wave at $f = pf_s$ amplitude-modulated by $g(t)$. None of the sidebands resulting from this modulation overlap $g(t)$ in frequency if $g(t)$ is confined to the Nyquist interval. It is well known that two signals are uncorrelated if their frequency bands do not overlap (but not, in general, otherwise).[14]

Dividing equation (109) by $\langle g^2 \rangle = R_g(0)$ gives the lemma in normalized form. The procedure given here is a slight generalization of one given by Bennett for $k = 0$ (see pp. 468–469 of Ref. 5).

REFERENCES

1. Laane, R. R., and Murphy, B. T., unpublished work. There have been other recent expressions of interest in ΔM-coded speech, namely, Tomozawa, A., and Kaneko, H., "Companded Delta Modulation for Telephone Transmission," IEEE Trans. Commun. Techniques, *16*, No. 2 (February 1968), pp. 149–157, and Brolin, S. J., and Brown, J. M., "Companded Delta Modulation for Telephony," IEEE Trans. Commun. Techniques, *16*, No. 2 (February 1968), pp. 157–162.
2. de Jager, F., "Deltamodulation, A Method of PCM Transmission Using the 1-Unit Code," Philips Res. Rep. 7, 1952, pp. 442–466.
3. van de Weg, H., "Quantizing Noise of a Single Integration Delta Modulation System with an N-Digit Code," Philips Res. Rep. *8*, 1953, pp. 367–385.
4. Wang, P. P., "Idle Channel Noise of Delta Modulation," IEEE Trans. Commun. Techniques, *16*, No. 10 (October 1968), pp. 737–742.
5. Rice, S. O., quoted in Bennett, W. R., "Spectra of Quantized Signals," B.S.T.J., *27*, No. 3 (July 1948), p. 466.
6. Korn, G. A., and Korn, T. M., *Mathematical Handbook for Scientists and Engineers*, Section 21.8-4, New York: McGraw-Hill, 1961.
7. Bennett, W. R., "Spectra of Quantized Signals," B.S.T.J., *27*, No. 3 (July 1948), p. 450.
8. Protonotarios, E. N., "Slope Overload Noise in Differential Pulse Code Modulation Systems," B.S.T.J., *46*, No. 9 (November 1967), pp. 2119–2161.
9. Cochran, W. T., and Lewinski, D. A., "A New Measuring Set for Message Circuit Noise," B.S.T.J., *39*, No. 4 (July 1960), p. 916.
10. French, N. R., and Steinberg, J. C., "Factors Governing the Intelligibility of Speech Sounds," J. Acoust. Soc. Amer., *19*, No. 1 (January 1947), p. 94.
11. Jolley, L. B. W., *Summation of Series*, New York: Dover Publications, 1961, p. 100.
12. Schouten, J. P., and van't Groenewout, H. W. F., "Analysis of Distortion in Pulse-Code Modulation Systems," Appl. Sci. Res., *B2*, (1951-52), pp. 277–290.
13. Rice, S. O., "Mathematical Analysis of Random Noise," B.S.T.J., *24*, No. 1 (January 1945), p. 51.
14. Bennett, W. R., *Electrical Noise*, McGraw-Hill Book Company, New York, New York, 1960, pp. 209–210.